The ATLAS Tile Calorimeter

A. Henriques, CERN, on behalf of the ATLAS Collaboration

***Abstract*- TileCal is the Hadronic calorimeter covering the most central region of the ATLAS experiment at the LHC. It uses iron plates as absorber and plastic scintillating tiles as the active material. Scintillation light produced in the tiles is transmitted by wavelength shifting fibres to photomultiplier tubes (PMTs). The resulting electronic signals from the approximately 10000 PMTs are measured and digitised every 25 ns before being transferred to off-detector data-acquisition systems. This contribution will review in a first part the performances of the calorimeter during run 1, obtained from calibration data, and from studies of the response of particles from collisions. In a second part it will present the solutions being investigated for the ongoing and future upgrades of the calorimeter electronics.**

I. Introduction

ATLAS is one the 2 multi-purpose experiments at the Large Hadron Collider (LHC) at CERN and has collected approximately 26 fb^{-1} of pp collisions in the period 2009-2012 with a center of mass energy 2.5, 7 and 8 TeV [1]. In 2013-2014 a long shutdown took place for a massive consolidation of LHC allowing to increase it's center of mass energy to 13 TeV. The first collisions with 25 ns bunch crossing are planned for summer 2015. During this long shutdown important consolidations were done in the ATLAS detector.

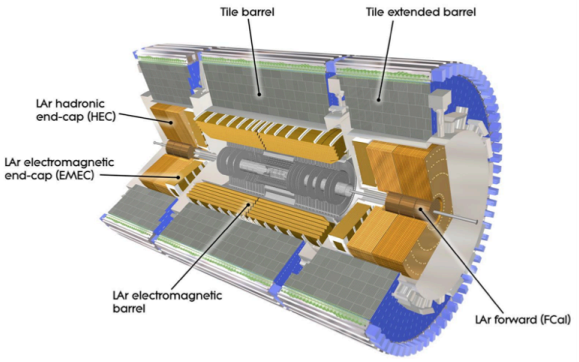

Fig. 1. A cut-away view of the ATLAS calorimeters. The Tile Calorimeter consists of one central barrel and two extended barrels.

Calorimeters represent an important component of the ATLAS detector, see Fig. 1. The electromagnetic (em) lead/liquid argon (LAr) calorimeter followed by the hadronic Tile calorimeter (Tilecal) cover the central region of the ATLAS detector up to a pseudorapidity[1] of $|\eta| < 1.7$, other LAr based calorimeters span across the forward regions, up to $|\eta| < 4.9$. Together with the em calorimeter, TileCal provides precise measurement of hadrons, jets, taus and missing transverse energy (E_T^{miss}) with a jet resolution $\sigma/E \sim 50\%/\sqrt{E}$ [GeV] $\oplus$ 3%, response linearity within ~ 1% up to few TeV energies and good E_T^{miss}.

TileCal has a fixed central barrel (LB), and two moveable extended barrels (EB). Each cylinder is composed of 64 modules, each covering the azimuthal ϕ angle of $2\pi/64 = 0.1$. It is made of alternating layers of iron plates and scintillating tiles. The scintillating tiles are placed in the plane perpendicular to the colliding beams and are radially staggered in depth, as illustrated in Fig. 2 [2]. The scintillating tiles are read-out by wave-length shifting (WLS) fibers on both sides of each module. These fibers deliver the light to photo-multipliers (PMTs) located in the outer radius iron structure that also houses the front-end electronics. Each cell is readout by 2 PMTs. The innovative tiles orientation of Tilecal, parallel to the incoming particles at η=0, allow the WLS fibres to run straight to the outer radius, allowing for a good calorimeter hermeticity and easy tiles-fibres coupling. The tiles, made by injection molding, are 3 mm thick and the ratio of iron to scintillator is 4.7 to 1, allowing for a good sampling frequency and a compact calorimeter with and effective nuclear interaction length λ = 20.7cm.

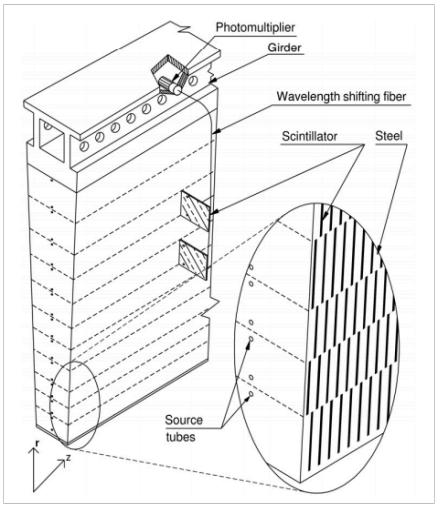

Fig. 2. Schematic showing the mechanical assembly and the optical readout of the Tile Calorimeter, corresponding to a φ wedge. The various components of the optical readout, namely the tiles, the fibres and the photomultipliers, are shown. The trapezoidal scintillating tiles are oriented perpendicular to the colliding beam axis and are read out by fibres coupled to their non-parallel sides.

[1] Pseudorapidity η is defined as $\eta = -\ln\tan(\theta/2)$, where θ is the polar angle measured from the beam axis. The azimuthal angle φ is measured around the beam axis, with positive (negative) values corresponding to the top (bottom) part of the detector.

ATL-TILECAL-PROC-2015-002
27 March 2015

The calorimeter modules are segmented into three longitudinal layers (A, BC, D) of 1.5, 4.1 and 1.8 λ in the barrel and 1.5, 2.6, 3.3 λ in the extended barrels, with a total calorimeter depth of 7.4 λ at η = 0 (9.7 λ when including the em calorimeter). Each cell has a transversal segmentation of Δη × Δφ = 0.1 × 0.1 (0.2 × 0.1 in the outer D layer). In addition to the regular cells, gap/crack scintillators have been installed in front of the Tilecal extended barrel and LAr electromagnetic end cap calorimeters, to improve the performance in this region occupied by many services and electronics from the inner tracker the LAr calorimeter.

In total, TileCal has approximately 5000 cells and 10000 channels. In the electronics readout, the signals from the PMTs are shaped and amplified in two gains with relative ratio 1:64. Each signal is digitized at a rate of 40 MHz and stored in the front-end pipeline memory. Upon arrival of a first level trigger accept, seven samples from the appropriate gain are sent to the back-end electronics for energy and time reconstruction. The amplitude of the signal is then reconstructed using an optimal filtering algorithm. The analog trigger summation is performed with cells in the same projective tower in order to provide a fast signal for the level-1 trigger.

The Tile Calorimeter is the result of a long process of R&D and prototype optimization using valuable feedback from test beams and simulation studies (1993-1995). The Technical Design Report has been completed in 1995, followed by the final construction in 1996-2004. The installation in the experimental cavern took place in 2004-2006, followed by the commissioning in 2007-2009 using cosmic muons. This was a long path to be ready and with excellent performance during the proton-proton collisions of 2009-2012 [2,3,4]. In the next sections some of the most relevant results will be presented as well as the planned upgrades for the future.

II. Performance in test beams and in LHC run 1

The main characteristics of Tilecal are summarized in table 1, obtained in test beams at CERN/SPS, using Monte Carlo (MC) simulations and measurements in the LHC run 1 data taking. The single hadron energy resolution obtained in test beams for Tilecal standalone is described by $\sigma_E/E(\pi) = 52\%/\sqrt{E} \oplus 5.7\%$ for an incident angle η=0.2, corresponding to an effective depth of 7.7 λ. The energy resolution for production modules displays a significant dependence on incident angle η, mostly as a result of the increase in effective depth and decrease of longitudinal leakage as η increases. The longitudinal leakage affects mostly the energy resolution of high energy particles and consequently reflects in the increase of the constant term. Results obtained in earlier test beams using Tilecal prototypes 1.5 λ deeper (to account for the final ATLAS calorimetry depth when the LAr em calorimeter is in place) give similar energy resolution scaling term but a constant term ~ a factor of 2 smaller, well described by $\sigma_E/E(\pi) = 45\%/\sqrt{E} \oplus 2.7\%$ (see table 1). Fig 3 shows the pion energy resolution as a function of the inverse square root of the beam energy obtained in the combined test beam with the LAr electromagnetic and Tile hadron calorimeters at |η| = 0.25. The measured energy resolution is well fitted by the sum in quadrature of a stochastic term of 52% a constant term of 3% and an electronic-noise term of 1.6 GeV. These experimental results and careful tuning of Monte Carlo allowed to anticipate a good jet resolution in ATLAS before collisions to be described by $\sigma_E/E(\text{MC jets}) = 64\%/\sqrt{E} \oplus 2.7\% \oplus 5.4\text{GeV}/E$.

TABLE I. TILE CALORIMETER MAIN CHARACTERISTICS AND PERFORMANCE

Ratio Steel/Scintillator	4.7:1
η coverage	|η|<1.7 (Barrel+2 Extended Barrels)
Longitudinal granularity	3 layers
Transversal granularity	ΔηxΔφ =0.1x0.1 (0.2x0.1 outer D layer)
Gain-dynamic range	10^5 ; 2 gain 10 bits ADCs
Nuclear interaction length	λ = 20.7cm
Moliere Radius	20.5 mm
Depth (at η=0)	7.4 λ (9.7 λ with LAr em calo+tracker)
Light yield	~70 photoelectrons/GeV
Sampling fraction (em)	2.7%
e/h	1.36
σ_E/E (π) Tilecal (7.7 λ)	$52\%/\sqrt{E} \oplus 5.7\%$
σ_E/E (π) Tilecal (9.2 λ)	$45\%/\sqrt{E} \oplus 2.7\%$
σ_E/E (π) Tile +LAr	$52\%/\sqrt{E} \oplus 3.0\% \oplus$ 1.6 GeV/E
σ_E/E jets MC (Tile+LAr)	$64\%/\text{SQRT E(GeV)} \oplus 2.7\% \oplus 5.4\text{GeV}/E$
Time resol. (collisions)	0.85 ns
Max. optics damage run 1	-2% (2.2 Krad in inner layer |η|~1.25)
Max. optics loss (HL LHC)	-15% (0.2-0.3 Mrad ; 3000 fb^{-1})

Figure 4 shows the measured ATLAS jet resolution in run 1 (2010) in the barrel region with different calibration methods. The measured jet resolution at high p_T is close to the design of 3% constant term. The presence of pile-up worsens the low p_T resolution. Improvements in the medium and low PT range crucially depend on pile-up corrections for in-time/out-time bunches, noise threshold tuning in LAr calorimeter and using inner tracker information.

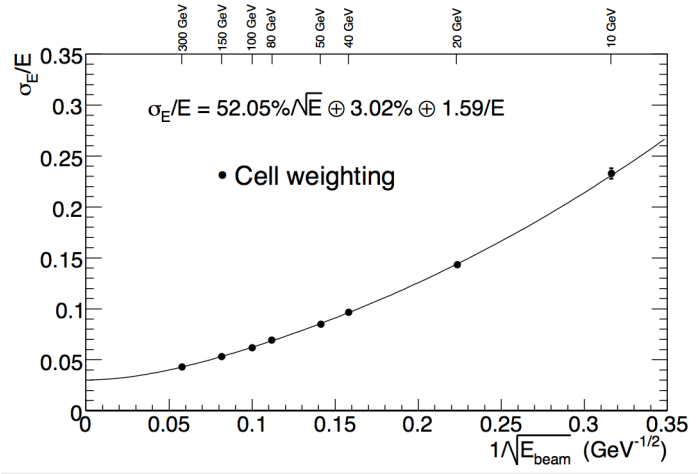

Fig. 3. Fractional energy resolution measured in test beams using pions as a function of the inverse square root of the beam energy, for combined LAr electromagnetic and Tile hadron calorimeters at |η| = 0.25. The curve corresponds to the result of a fit to the data points [1].

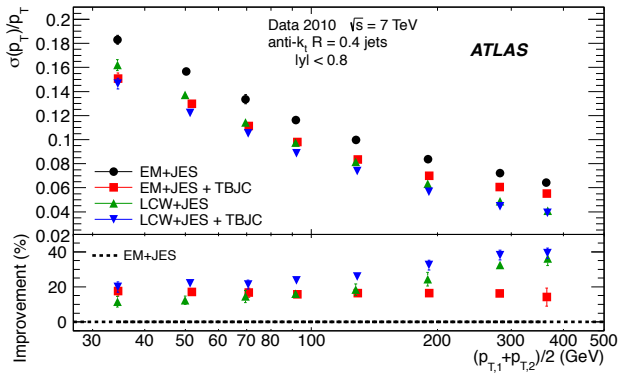

Fig. 4 ATLAS fractional jet resolution as a function of the jet p_T for different calibration schemes, measured in 2010 data for anti-kt jets with a cone radius R= 0.4 and for four jet calibration schemes. The lower part of the figure shows the relative improvement of the various calibrations with respect to the EM+JES jet calibration scheme where jets are only calibrated at the electromagnetic scale. The errors shown are only statistical.

Keeping all the Tilecal cells always calibrated at the electromagnetic scale during the life of the ATLAS experiment at the % precision level is an important parameter to keep a good jet and missing transverse energy performance and in particular to achieve a jet energy scale (JES) uncertainty at the 1-2% level. The JES error is in fact the main uncertainty contribution in many ATLAS physics results (jet/dijet cross section, top, etc). This uncertainty is illustrated in Fig. 5 as a function of pseudorapidity for jets P_T = 300GeV. In the central η region the uncertainty is ~ 1%.

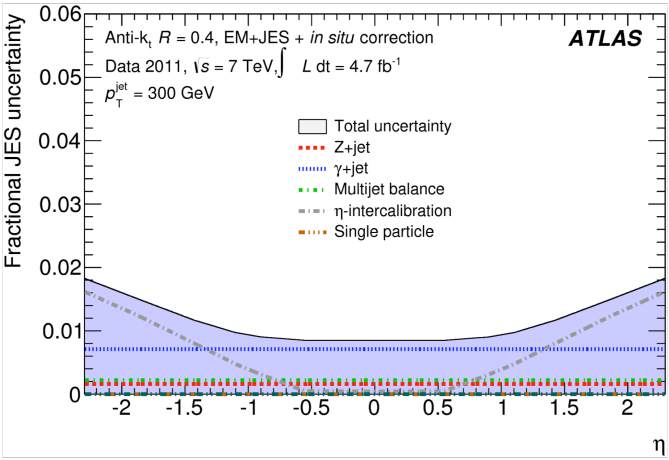

Fig. 5 Fractional in situ jet energy scale (JES) systematic uncertainty as a function of jet pseudorapidity for anti-kt jets with distance parameter of R = 0.4 calibrated using the EM+JES calibration scheme. The contributions from each in situ method are shown separately.

In 2001-2003 11% of the TileCal modules were calibrated at the beam tests. Electron beams with energies between 20 and 180 GeV were used to establish the electromagnetic scale for the first calorimeter layer, while the two other longitudinal layers were inter-calibrated with respect to the first one using muons. The average em scale factor of 1.05 pC/GeV was obtained with an RMS spread over the tested cells = 2.4%, mostly dependent on the optics non-uniformity.

After installation of the whole Tilecal modules in the ATLAS experimental cavern the cells inter-calibration was done using three gamma ^{137}Cesium sources [5], one per cylinder. They move through every Tile scintillator inside the cells allowing to calibrate the optics, PMT and the electronics chain. The high voltage of every PMT was adjusted to have the cell response to cesium equal to the response measured during beam tests with the same cesium calibration system. The comparison between cosmic muon data acquired during the commissioning of the overall detector, muons from test beams and Monte Carlo (MC) predictions has confirmed that propagation of the electromagnetic scale from the beam tests to ATLAS was successful. As seen in Fig. 6 the non-uniformity within one layer is ~ 2-3% and the maximal difference between layers is 4%. Cosmic muon data was acquired during each yearly shutdown and in periods when there is no LHC data taking.

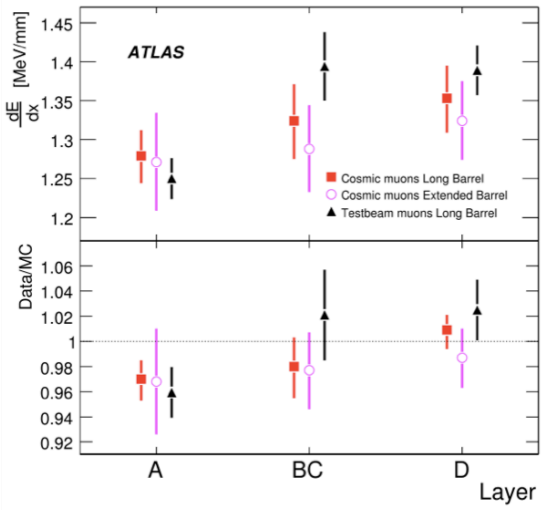

Fig. 6. The truncated mean of the dE/dx for cosmic data taken in 2009 and test beam muons shown per radial compartment and, at the bottom, compared to Monte Carlo. The error bars shown combine in quadrature both the statistical and the systematic uncertainties.

In addition, during data taking in-situ methods are used to check the Tilecal electromagnetic scale stability and precision, such as e/p method, response of muons from collisions (W—>μν). Fig. 7 shows the mean value of the ratio between the energy deposited in Tilecal and the track momentum measured by the inner tracker as a function of η, showing a very good agreement with MC. The maximum deviation data to MC is 10% in the region |η| ~ 1, corresponding to the gap region between the barrel and the extended barrel. All these methods allow us to confirm that after applying the proper calibration corrections, described in detail in the next section, the electromagnetic scale is stable over several years period, being it's precision ~3%.

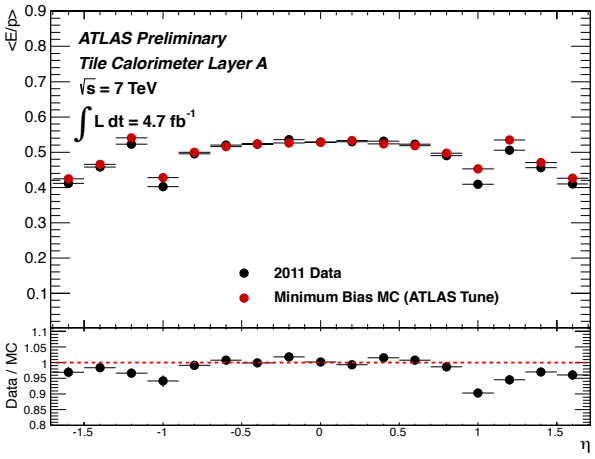

Fig. 7 Mean value of the ratio of the e/p ratio in the Tile calorimeter vs η during 2011 LHC collisions in ATLAS.

III. TILECAL CALIBRATIONS AND OPERATIONS IN RUN 1

During run 1 the main Tilecal calibration relies on the cesium calibration system [5], already used during test beams to transport the electromagnetic scale of all the Tilecal cells (see previous section). The Cesium source (~ 10mCi) scans all the cells, over approximately 20 km of pipes located inside the scintillating tiles 1 to 2 times per month, when there is no LHC beam. This system monitor the overall response of scintillating tiles, fibres and PMTs. Any deviation from the expected decay rate of -2.3% /year is corrected offline, keeping all the cells calibrated at the em scale while maintaining the High voltage delivered to the PMTs unchanged during run 1. Fig. 8 shows the global cells drifts in 2012, between the start and end of the proton collisions period as function η, for the three calorimeter layers. The bigger signal reduction is ~ -3% and is observed in the inner most layer at $|\eta| = 1.25$ (cell A13). This is the region where the depth of em LAr calorimeter barrel sitting in front of Tilecal is smaller, due to the gap between the barrel and the end-cap em LAr calorimeters (see Fig. 1).

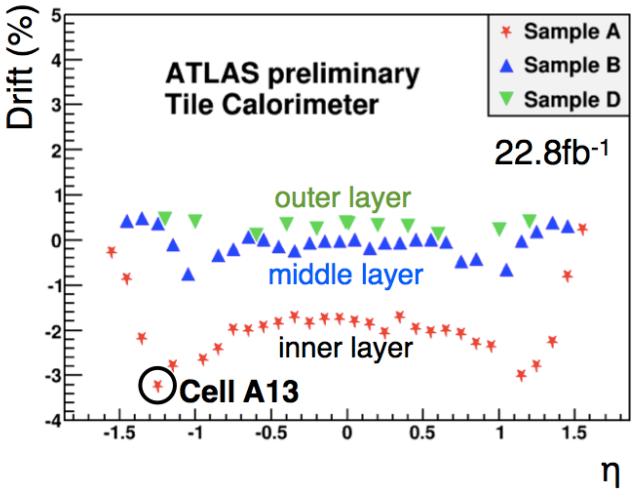

Fig. 8 The Tile Calorimeter maximal variations in 2012 for the 3 longitudinal layers as a function of η, using the cesium calibration system.

Other complementary calibration systems (laser, CIS and Mbias) monitor each component of the calorimeter. The Laser calibration makes use of short calibrated laser pulses that are sent directly to all PMTs. The laser monitor the stability of the PMT gain between two Cesium calibrations. It also allows testing the response of the digital readout electronics. The CIS injects a known electric charge into the readout electronics chain, simulating a PMT output pulse. It monitors the linearity of the ADCs and measures the conversion factor from ADC counts to pico-Coulomb (pC). Laser and CIS runs are taken about twice a week. The signal produced by minimum bias (Mbias) events are used to monitor the overall changes in Tilecal as the cesium system, after unfolding the Luminosity changes over time.

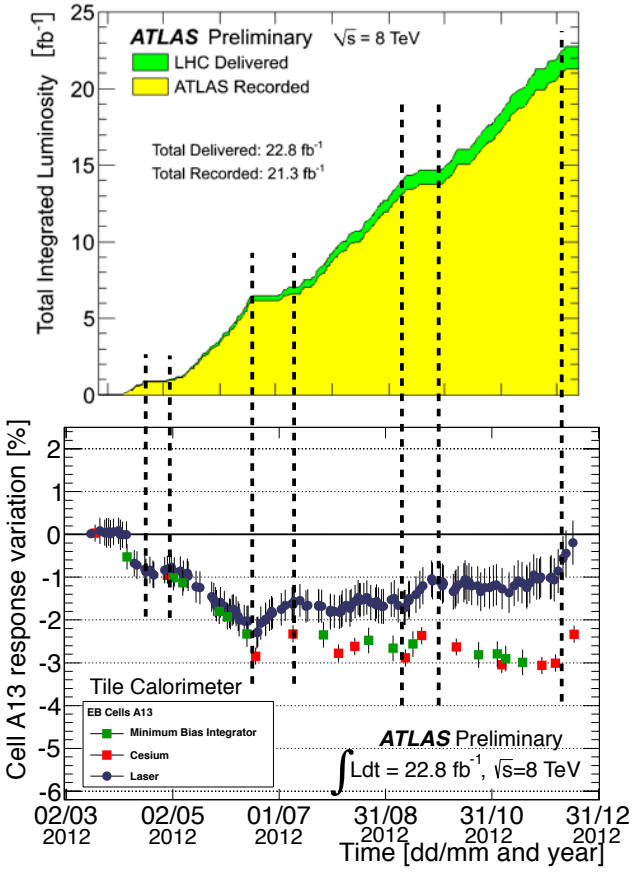

Fig. 9 (Top) The evolution of ATLAS total integrated luminosity in 2012. (Bottom) The evolution of the response of the most exposed Tilecal inner layer cell (A13) located at $|\eta| = 1.25$ as a function of time in 2012. The response is measured by the Cesium, the Laser and the Minimum Bias calibration systems. The measurements are normalized to the first run taken in 2012. Periods with no collisions are delimited by vertical dotted lines.

Comparing the results of the various calibration systems, for the most exposed Tilecal regular cell (A13), see Fig. 9, we observe that the PMTs gain variations, monitored with the laser are the main source of the cells drifts. The PMTs down-drifts coincide with the periods of data, while the up-drifts (PMT gain recovery) coincide with the technical stops (no beam). At the end of the 2012 proton-proton collisions period the PMTs gain variation in A13 was ~ -1% and the radiation-

induced signal loss in the scintillator tiles/fibres was ~ -2%, as seen by the difference between the loss observed by the cesium and laser response. In 2011 no radiation damage was observed in the optics components. The information extracted from the Mbias calibration system is in good agreement with the cesium information. The maximum accumulated dose expected in A13 in run 1 is ~ 2.2 krad for ~ 25fb^{-1} delivered luminosity. The scintillator damage observed is within errors in good agreement with expectations, based on laboratory measurements on irradiated optics components. At the end of the HL-LHC run (3000 fb^{-1}) we expect in the most exposed (A13) cell a maximum of -15% losses due to scintillator damage for a total dose of ~ 0.2 – 0.3 Mrad. The follow-up of the damage during run 2 will allow to confirm these expectations. Overall, the major source of short term changes in Tilecal cell response is due to the PMTs gain variations, which are corrected, if necessary with a laser calibration system in between two cesium runs. The stability of the electronics behind the PMTs is inferred with the CIS calibration system, showing a very good stability of ~ 0.4% during 2012 running.

Pile-up is a concern at the LHC, coming both from the same bunch crossing as the triggered one (in time pile-up) or from previous bunch crossings (out of time pile-up). In time pile-up is observed as an increase of the cells noise, which increases with the average number interactions per bunch crossing μ. Figure 10 shows the cell noise induced by pile-up as a function μ for each layer of Tilecal, showing an approximately linear increase with pile-up. In the most affected inner radius layer A, the pile-up noise is around 55 MeV for an average μ = 17.

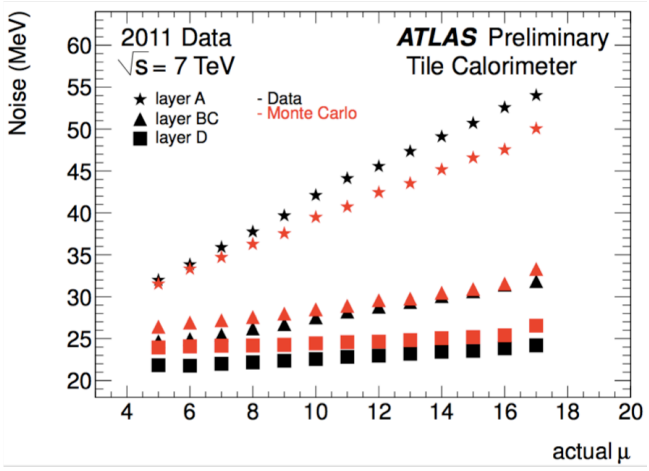

Fig. 10 Pile-up noise in Tilecal cells as a function of the average pile-up (μ) in the three longitudinal layers of the calorimeter. Results are shown for data and MC.

The precision of the measured Tilecal signal time is important to discriminate between in-time and out-of-time collisions and to optimize the cell energy reconstruction. The time resolution on the Tilecal cells is very good, 0.85 ns for jets and muons with deposited energy above few GeV, see Fig. 11.

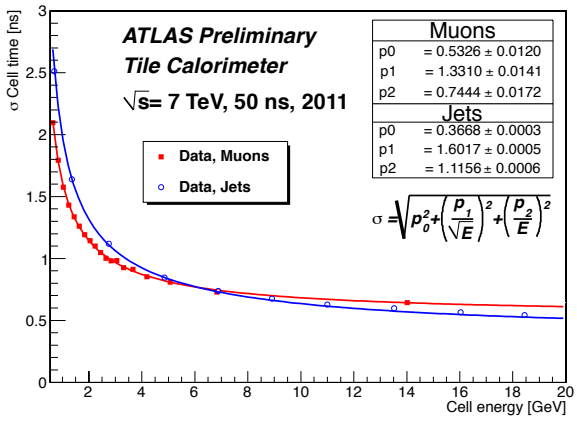

Fig. 11 Tilecal cell time resolution as a function of energy deposited in the Tilecal cells by jets and muons.

One of the main problems encountered during the TileCal operation was the occurrence of very frequent trips of the low voltage power supplies (LVPS), with a total of approximately 14000 trips in 2012 and with a very strong correlation to the integrated luminosity. Automatic procedures were implemented in run 1 in order to monitor and recover the modules within a few tens of seconds after a trip. A new design of the LVPS has been developed. 38 new units (15% of the total needed) were installed in the calorimeter during the yearly shutdown of 2011. They were tested in real conditions during the 2012 data taking, showing only 1 trip in 2012. Consequently all LVPS have been replaced by news ones in the 2013-2014 shutdown, expecting a drastic reduction in the number of tripped modules in run 2. With the newest version of the LVPSs, a significant reduction of the electronic noise is observed and the noise distribution becomes more Gaussian. The electronics cell noise measured in random trigger runs is around 20 MeV with the new LVPS, see Fig 12. These improvements will further improve the resolution for physics analysis which rely on Tilecal.

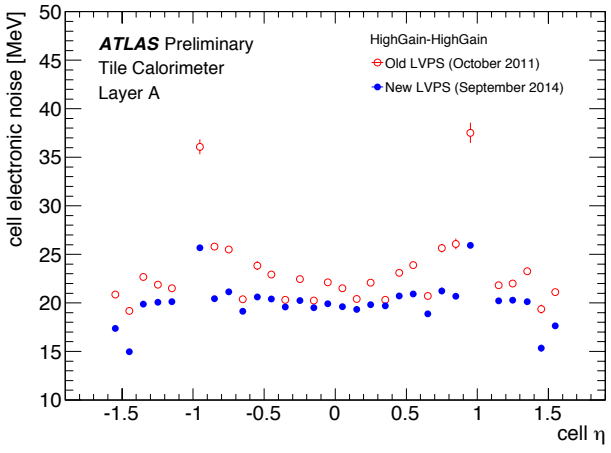

Fig. 12 Electronic noise (defined as the RMS of the pedestal) in MeV as a function of cell η. The two periods in comparison are October 2011, when an older version of the LVPSs was installed, and September 2014, after the long shutdown consolidation campaign and installation of newer LVPSs. Only cells of the layer A are shown.

In addition to the full replacement of the Low Voltage power supplies, Tilecal used the 202-2014 shutdown to make major consolidation of the on-detector readout electronics, in particular to reinforce weak electrical connections inside the front-end electronics, the second major source of hardware failures in run1. Figure 13 shows the fraction of masked cells over time since 2010, increasing during the periods when the LHC was operational and decreasing to almost 0% during the maintenance periods when the front-end electronics could be accessed and repaired. These mentioned consolidations should reduce the amount of cells that are masked during data-taking due to a malfunctioning of the hardware and ensure high performance, high quality and robust operations during Run 2.

Despite the few % Tilecal cells masked every year during data taking, the data quality efficiency for TileCal alone was more than 99% with the main sources of inefficiency being problems with timing and with the readout system.

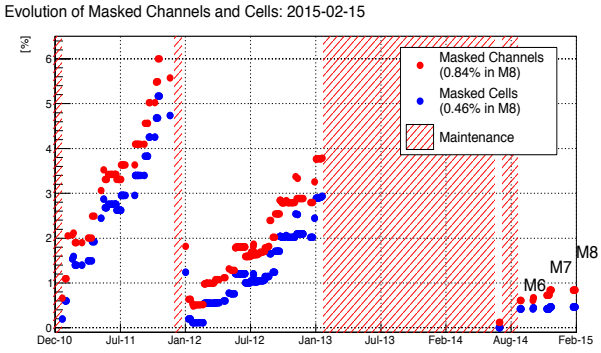

Fig. 13 Percentage of masked TileCal cells as a function of time, from December 2010 to February 2015. A sharp increase in the fraction of masked cells corresponds to the loss of an entire module, for example due to failures in the LVPS. The sudden decrease at the end of 2011, 2012 and summer 2014 correspond to maintenance periods, when the front-end electronics could be accessed and repaired.

During the 2012-2014 shutdown the outermost D layer cells (D5 and D6) of the Tilecal extended barrel are being integrated in the level 1 (LV1) muon trigger, together with the end-cap muon trigger chambers. This will reduce significantly muon fake rates originated from the slow charged particles (protons) in the region $1.0 < |\eta| < 1.3$ while maintaining a good muon efficiency. Figure 14 shows the muon detection efficiency and muon fake reduction as a function of the energy threshold applied to the D5+D6 Tilecal cells energy, obtained with a prototype receiver module connected to the Level-1 calorimeter trigger electronics during run 1. 50 ns runs were used to collect good muon tracks (black dots) and 25 ns runs were taken to calculate the fake trigger rate with the slow particles coming from the previous bunch (red triangles).

The final Tile muon digitizer board, which will process the calorimeter analogue signals from all the outer layer extended barrel cells and will provide the coincidence flags, is under construction. It should be installed and commissioned before the 25 ns proton collisions expected in summer 2015.

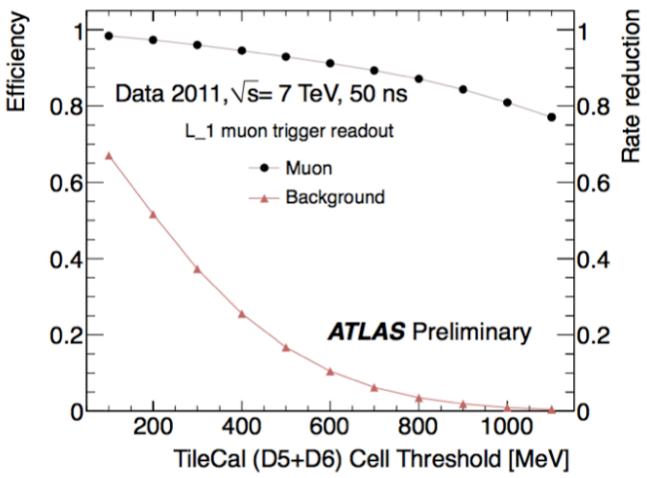

Fig. 14 Muon detection efficiency and background reduction using a prototype receiver module connected to the Level-1 calorimeter trigger electronics during run 1. 50 ns runs were used to collect enough good muon tracks (black dots) and calculate the muon efficiency. 25 ns runs are taken to calculate the fake trigger rate rate reduction with the slow particles coming from the previous bunch (red triangles).

IV. FUTURE UPGRADES

The upgrade plans of the high Luminosity LHC foresee an increase of the instantaneous luminosity from 10^{34} $cm^{-2}s^{-1}$ to 5-7 × 10^{34} $cm^{-2}s^{-1}$ in two steps. A long shutdown will take place in 2018 (phase I) and 2023 (phase II). During the Phase I upgrade Tilecal will replace only the gap/crack scintillators due to radiation damage, as planned since the initial detector construction.

For the Phase II upgrade, a major upgrade of the Tilecal front end and back end electronics is planned. The PMTs will not be changed but all other readout electronics components will be replaced with an architecture allowing sending at 40 MHz all the samples to the off-detector electronics. This will allow a fully digital trigger implementation, with more sophisticated trigger algorithms to compensate for the more complex backgrounds expected at high luminosity. Since the front-end electronics is not accessible without opening the detector more redundancy and fail safe operation have been important issues taken in consideration when re-designing the new electronics system.

To gain experience with the new design, a demonstrator project has been initiated, aimed at installing and running a prototype of the upgraded electronics in test beams at the end of September 2015 and installation in the ATLAS Tile calorimeter at the next shutdown. Since the upgraded electronics is expected to have smaller noise and full digital readout for the Level-0 triggers, all the Tilecal outermost D layer cells, including the barrel can be integrated in the muon L0 trigger in combination with MDT, RPC and TGC chambers. The calorimeter provides nearly hermetic coverage for muon detection in ϕ and within $|\eta| < 1.4$. The overall efficiency for detection of a muon with $pT > 10$ GeV is expected to be better than 98% when the fake 17 rate less than 13%. The Tile calorimeter is capable of efficiently

suppressing non-collision backgrounds to muon triggers. This is illustrated in Fig. 15, showing the distributions in η of regions of Interest (RoIs) from level 1 muon triggers with p_T >10 GeV (L1_MU10) before (solid black line) and after applying the Tile D layer coincidence (shaded red histogram).

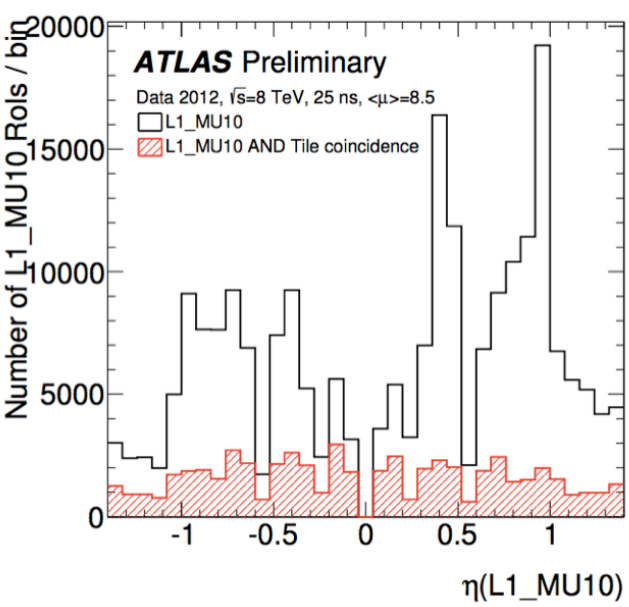

Fig. 15 The distributions in η of regions of Interest (RoIs) from level 1 muon triggers with p_T >10 GeV (L1_MU10). The distributions are before (solid black line) and after applying the Tile coincidence (shaded red histogram). The energy D cell threshold for the coincidence requirement is 150 MeV.

V. CONCLUSIONS

The ATLAS Tile Calorimeter has been performing very well during 2009-2012 LHC run1, achieving a high data quality efficiency and good performance. During the 2013-2014 shut-down major interventions were taken to replace all the low voltage power supplies, reinforce weak electrical connections inside the frontend electronics and integrate the Tile outermost layer of the extended barrel in the LV1 muon trigger to remove muon fake rates. These actions should ensure that the Tile calorimeter will be in the best conditions for the first collisions of run2.

REFERENCES

[1] The ATLAS Collaboration, The ATLAS experiment at CERN Large Hadron collider, JINST 3:S08003, 2008

[2] Tile Calorimeter Technical Design Report, CERN/LHCC/96-42

[3] P. Adragna et al. Testbeam studies of production modules of the ATLAS Tile Calorimeter, Nucl. Instr. Methods A 606, 362-394 (2009)

[4] G. Aad, et al., Readiness of the ATLAS Tile Calorimeter for LHC collisions, EPJC-Particles and Fields 70 (2010) 1193–1236

[5] E. Starchenko et al. Cesium monitoring system for the ATLAS Tile Hadron Calorimeter. *Nuclear Instruments and Methods*, A494:381–384, 2002.